Assessment of Thalamic Perfusion in Patients with Mild Traumatic Brain Injury by True FISP Arterial Spin Labeling MR Imaging at 3T

Yulin Ge, **Mayur B. Patel**, **Qun Chen**, **Elan Grossman**, **Ke Zhang**, **Laura Miles**, **James S. Babb**, **Joseph Reaume**, and **Robert I. Grossman**
Center for Biomedical Imaging, Department of Radiology, New York University School of Medicine, New York, NY, 10016, USA

Abstract

Functional blood flow abnormalities after brain injury have been demonstrated in animal models of head trauma and are considered to contribute to post concussive syndrome (PCS). In order to better characterize cerebral blood flow (CBF) changes and PCS in patients with mild traumatic brain injury (MTBI), we determined CBF in different brain regions using a true fast imaging with steady state precession arterial spin labeling (True FISP ASL) imaging at 3T. We also investigated the severity of neuropsychological functional impairment with respect to hemodynamic changes. Twenty-one patients with clinically diagnosed MTBI and 18 healthy age-matched controls were studied. The median time since the onset of brain injury in patients was 26.5 months. True FISP ASL MRI was performed at 3T MR in which a flow-sensitive alternating inversion recovery (FAIR) preparation was applied. Measurements of regional CBF were made in both deep gray matter including thalamus and white matter at the basal ganglia level. The mean regional CBF was reduced and more significantly in both sides of thalamus in patients with MTBI (45.9±9.8ml/100g/ min) as compared to normal controls (57.4±10.3ml/100g/min; p=0.002). The decrease of thalamic CBF was significantly correlated with several computerized neuropsychological measures including processing and response speed, memory, verbal fluency, and executive function in patients with MTBI. These results indicate that hemodynamic impairment can occur and persist in patients with MTBI, the extent of which is more severe in thalamic regions and correlate with neuropsychological impairment during the extended course of the disease.

Keywords

Mild traumatic brain injury; cerebral blood flow; ischemia; thalamus; magnetic resonance imaging; arterial spin labeling

INTRODUCTION

Mild traumatic brain injury (MTBI) accounts for at least 75 percent of all traumatic brain injuries and is often associated with long-lasting post concussive syndrome (PCS). Patients with MTBI may initially experience transient loss of consciousness or a brief amnestic period with disabling physical (headache, dizziness, fatigue, noise and light sensitivity), cognitive (memory, attention, concentration, executive function deficits), and emotional/ behavioral (depression, anxiety, irritability) sequelae that can persist for months or years

Address correspondence and reprint requests to: Dr. Yulin Ge, MD, Center for Biomedical Imaging, Department of Radiology, New York University School of Medicine, 650 First Avenue, 6th floor, Rm 615, New York, NY 10016 USA, yulin.ge@med.nyu.edu, Phone: (212) 263-3784, Fax: (212) 263-7541.

following mild injury [1]. There is an increasing awareness of an epidemiologically large but silent presence of MTBI as well as its serious, long-lasting consequences in the recent years, however, the pathophysiological mechanism of MTBI and PCS is still poorly understood and it is not possible to detect patients at risk of developing PCS on the basis of clinical presentation [2]. In addition, biological markers of MTBI are still missing and little imaging evidence exists for the organic origin of postconcussional disorder [3, 4].

The vast majority of literature on TBI is concerned with the investigation of abnormalities in classic regions that have been described in animal models and those observed in moderate to severe cases of TBI in humans. Thus, it is believed that brain pathology in MTBI is the result of diffuse axonal injury (DAI) occurring predominantly in stereotypical locations such as the gray-white junction, the splenium of the corpus callosum, and the midbrain [5]. However, the influence of injury to the thalamus, a complex deep grey matter mass that consists of many groups of nuclei and white matter bundles which are vulnerable to damage during sudden acceleration or deceleration of the brain, has been poorly investigated. As the central relay station for transmitting information throughout the brain, the thalamus is important to communication among sensory, motor, and associative brain regions [6–9], suggesting that damage to this structure may affect multi-functional pathways and potentially long-term morbidity associated with persistent PCS.

Since viable brain tissue is highly dependent on its oxygen supply, there is also accumulating evidence which indicates that regional ischemia plays a role in secondary brain injury in patients with brain trauma [10–14]. Studies on a wide variety of rodent models of brain trauma have shown reduced regional blood flow in the acute phase of injury [15–18]. In these laboratory models of moderate or severe traumatic injury, hypoperfusion is not only seen near the impact site but can also be widespread and distant [17, 19–23]. Although such brain perfusion abnormalities have been observed to be present at 1 week, delayed assessment on the order of months or years has been rarely carried out. Recently, using the controlled cortical impact (CCI) model in rats, Kochanek et al. [24] reported blood perfusion impairment with delayed cognitive deficits at one year, suggesting a long-term effect of CBF on TBI.

Most previous investigations of blood perfusion have used nuclear medicine techniques (PET, SPECT, Xe-CT) or dynamic susceptibility contrast enhanced MRI to study cerebral blood flow (CBF), which are limited by their low spatial resolutions as well as by their use of exogenous endovascular contrast agents. In the current work true fast imaging with steady state precession arterial spin labeling (true FISP ASL) [25] was employed for the measurement and quantification of local cerebral perfusion. True FISP ASL is an MRI method of investigating CBF that uses blood water as an endogenous, freely diffusible tracer and yields high resolution images without distortion artifacts or the need for exogenous endovascular contrast agents [26].

In this study, we applied true FISP ASL at 3T to test the hypothesis that there is hemodynamic impairment in the thalamic regions of patients with MTBI in a nonacute phase. We also investigated the correlation between the perfusion changes in these regions and neuropsychological dysfunction.

MATERIALS AND METHODS

Theory

High-field (3T) MR ASL perfusion imaging is appealing not only because of the advantage that it provides by increasing the signal-to-noise ratio (SNR), but also because it offers a greater T1 relaxation time for spin labeled arterial blood water [27–30]. Most pulsed ASL

methods are based on EPI, which is prone to distortion artifacts and rapid dephasing caused by local magnetic field inhomogeneities, especially at high fields. However, in true FISP ASL [25], a flow-sensitive alternating inversion recovery (FAIR) ASL [29] perfusion preparation is used in which the EPI sequence is replaced with a true FISP steady state precession data acquisition strategy. The benefits of such a sequence include high spatial resolution images with none of the distortion artifacts commonly associated with EPI based methods of ASL [26].

In true FISP ASL, slice-selective and slice-nonselective inversion pulses are used to generate a set of respective control and labeled images. In the control image the spins of tissue water contained in the spatially selective slice are inverted and in a different magnetization state from the fully relaxed inflowing arterial blood water located proximal to this region. In the labeled image, however, since it is acquired after a non-selective global inversion pulse that includes spins distal to this region, both blood and tissue water in the selective slice are in identical magnetization states. The control and labeled images are subtracted to produce an ASL difference image in which the signal from the static spins cancel each other out leaving a signal difference map of arterial blood delivered to each voxel during the interval TI. This signal difference map provides a qualitative measure of local perfusion from which CBF can be calculated.

To eliminate magnetic inhomogeneities due to residual contamination from static tissue, a frequency offset corrected inversion (FOCI) pulse was applied every 5 seconds [31–33]. The FOCI pulse had a slice thickness of 2.5 times the thickness of the imaging slice to compensate for imperfect slice profile. In order to correct for the imperfect subtraction of stationary tissue between control and labeled images due to off-resonance effects, an approach described by Figueiredo et al. [34] was adapted in which an extra pair of images was acquired at a very short inversion time ($TI_0 = 100$ ms), when no perfusion effects were expected. In order to determine the equilibrium magnetization of tissue (M_0), another separate scan was performed using the same true FISP sequence, but in the absence of an inversion-recovery preparation. In addition, the transit delay time for perfusion quantification, was also determined in one subject in which ASL data were collected at multiple TI times. These data were fitted to a general kinetic model described by Buxton et al. [35] and Yang et al. [31] for the estimate of the transit delay time.

The absolute perfusion in localized areas of deep gray matter were quantified using a general kinetic model described by Buxton et al. [35] and Yang et al. [31], as well as T1 values obtained from published works [32, 33]. Briefly, the signal difference (ΔM) between labeled and control images is given by:

$$\Delta M(t) = 2M_{0b}f\int_0^t c(t')r(t-t')m(t-t')dt' \quad (1)$$

where c(t) is the delivery function, r(t) is the residue function, m(t) is the magnetization relaxation function, M_{0b} is the equilibrium magnetization of arterial blood per unit mass of tissue, and f is CBF expressed in the units of ml of blood per ml of voxel per unit time. Using the standard kinetic model [30] for pulsed ASL equation 1 is reduced to:

$$\Delta M(t) = \begin{cases} 0 & 0<t<\Delta t \\ 2M_{0b}f(t-\Delta t)\alpha e^{-t/T_{1b}}q_p(t) & \Delta t<t<\Delta t+\tau \\ 2M_{0b}f\tau\alpha e^{-t/T_{1b}}q_p(t) & t>\Delta t+\tau \end{cases} \quad (2)$$

where Δt is the transit delay (time required for tagged blood to arrive at an imaging voxel), τ is the duration of the tagging bolus, T_{1b} is the longitudinal relaxation time of blood, $q_p(t)$ is a

dimensionless term that depends on Δt, τ, T1, and α represents tagging efficiency. When a FAIR perfusion preparation is used, the duration of the tagging bolus τ is very long compared to the inversion time TI of 1200 ms and CBF (f) can be derived from equation (2) as:

$$f = \frac{\Delta M}{2M_{0b}(TI - \Delta t)\alpha e^{-TI/T_{1b}}q_p(TI)} \approx \frac{\Delta M}{2M_{0b}(TI - \Delta t)\alpha e^{-TI/T_{1b}}} \quad (3)$$

Equation (3) was used for perfusion quantification in all subjects, in which M_{0b} was determined from a separate multi-TI inversion recovery scan and a Δt of 350 ms was used according to the method of Buxton et al. [35]. A T_{1b} = 1664 ms [36] and α = 1 were assumed for all subjects. Since $q_{p(t)}$ typically has a value close to one it was dropped from the equation.

Subjects

Twenty-one MTBI patients who had a history of head trauma and initial Glascow Coma Scale (GCS) score of 13 to 15 were studied on a whole body 3.0T MR. All the patients have symptoms that meet the criteria of the DSM-IV-TR classification for the diagnosis of postconcussional disorder. The median duration after onset of brain injury was 26.5 months (ranging from 8 months to 7 years). Patients were excluded when a previous diagnosis other CNS disorders was made including depressive disorder, alcohol abuse, somatic disorder stroke, epilepsy, and psychosis. Eighteen age-matched healthy controls without history of head injury were also recruited from the general population and scanned for comparison. All study protocols were conducted within the guidelines from the Institutional Review Board and consent was obtained from each participant.

MR Imaging and Image Analysis

All imaging experiments were implemented on a 3-T Siemens Trio whole-body MR scanner (Siemens Medical Systems, Erlangen, Germany) that operated with a maximum gradient strength of 45 mT/m and a slew rate of 200 mT/m/msec along all three axes. After conventional MR imaging, a high spatial resolution ASL perfusion MRI was acquired. An 8-element receiver head coil was used with body coil excitation. Data acquisition was made from 6 mm thick slice that was positioned parallel to the AC-PC plane at the level of the basal ganglia. Sequence parameters for a true FISP steady state precession readout were applied which included a flip angle (FA) of 50 degrees, a TR/TE of 5000 ms/1.64 ms, an image matrix size of 256×256, a field of view (FOV) of 220×220 mm^2, a pixel bandwidth of 975, and a TI of 1200 ms for both the slice-selective and slice non-selective inversion pulses and used to acquire the control and labeled images, respectively. However, in order to correct for the imperfect subtraction of stationary tissue between control and labeled images due to off-resonance effects, an approach described by Figueiredo et al. [34] was adapted in which an extra pair of images was acquired at a very short inversion time (TI_0 = 100 ms), when no perfusion effects were expected. To determine the equilibrium magnetization of tissue (M_0), another separate scan was performed using the same true FISP sequence, but in the absence of an inversion-recovery preparation. Another important parameter needed for perfusion quantification, the transit delay time, was determined in one subject in which ASL data were collected at multiple TI times. These data were fitted to a general kinetic model described by Buxton et al. [35] and Yang et al. [31] for the estimate of the transit delay time. The total imaging time for acquiring data using true FISP ASL was about 6.5 minutes.

Region of interests (ROIs) were made first on spin unlabeled or control image (TI=1200), and then copied to other corresponding images in order to obtain the matched size and

location for measuring the signal intensities from thalamus, putamen, the head of caudate nuclei, as well as in frontal white matter in each hemisphere in patients and controls were acquired using Image J (Image Processing and Analysis in Java. Available at: http://rsb.info.nih.gov/ij/).

Neurocognitive Testing

For neurocognitive tests, both patients and controls underwent a traditional consensus battery, which was applied within 12 hours of MRI examination and yielded measures of executive functioning, abstract reasoning, attention, concentration, verbal ability, psychomotor ability, and memory. This battery was comprised of eleven tests in seven neuropsychological functional categories, including Verbal Abstract Reasoning (Similarities Category and Similarities Shift), Attention and Concentration (Weinberg Visual Cancellation Test, Number Recall and Number Sequencing), Executive Functioning (Stroop), Verbal Fluency (FAS), Processing Speed (Animal Decoding and Symbol Scanning), Response Speed (Response Direction 1 and Response Direction 2), and Memory/Learning (Memory Cabinet 1 and Memory Cabinet 2). These are a set of computerized neurobehavioral measures that are suited for repeatable testing, are sensitive to regional brain dysfunction.

Statistical Analysis

The mean and standard deviation (SD) of each measure among patients and controls and the p value for the comparison of patient to controls in terms of each CBF and neuropsychological measure were computed using an unequal variance t test (T). All p values are two-sided and were not subjected to a multiple comparison correction. Spearman rank correlation was used to analyze the association of each neuropsycholgoical test with CBF of each side and averaged over the sides of each brain region across the patients. An uncorrected p value of 0.05 or less is considered significant.

RESULTS

There were no significant differences of age (P=0.35) and years of education (P=0.30) between patients with MTBI and healthy controls (34.1±8.6 *vs* 37.1±10.7 years old, 15±2.5 *vs* 16.1±3.8 years of education, respectively) with respect to the relevant measures assessed by an unequal variance t test. The two groups were also matched for gender. Traumatic brain parenchyma lesions were detected on conventional MR imaging including gradient echo imaging as well as T2- and T1-weighted imaging in only two patients, and they are small and in frontal and temporal regions. However, there were no visible lesions in basal ganglia region including thalamus in any of these patients.

The comparison of patient to controls in terms of CBF measure in each region was assessed and the mean and standard deviation (SD) values of CBF in each region among patients and controls are listed in Table 1. Patients with MTBI demonstrated significant lower CBF in thalamic region (both sides) than normal controls (P 0.002) (Fig. 2) with mean and SD values of CBF in right, left, and both sides (average) of thalamus in patients (46.9±10.4, 45.0±9.7, 45.9±9.8, respectively) and in controls (59.7±13.3, 55.2±9.7, 57.4±10.4, respectively). The CBF in the head of caudate nuclei was also significance (right side: P = 0.03 and both sides: P = 0.02) and near significance (left side: P = 0.06). While in other deep gray matter regions and frontal white matter regions, there was no statistical significant difference of CBF between the patients and controls.

For comparison of neuropsychological functions in patients and controls, eleven neuropsychological tests were performed that yield measures of executive functioning,

abstract reasoning, attention, concentration, verbal ability, psychomotor ability, and memory and expressed as standardized z score as shown in Table 2. Overall, patients with MTBI have a poor performance in these neuropsychological tests as compared to normal controls. Among the ten neuropsychological tests, the two groups differ significantly from each other on 5 of them including processing speed, response speed, cancellation error, verbal fluency (FAS), and executive functioning (Stroop) tests. These results confirmed that there is a neuropsychological functional impairment in patients with MTBI during the expanded course of the disease.

In patients with MTBI, we have assessed the correlations between the decreased blood perfusion (CBF) in thalamic regions (averaged from both sides) and neurocognitive parameters expressed as standardized z score. Table 3 presents the correlation coefficient (adjusted R^2) that reach the statistical significant levels (P 0.01) between thalamic CBF and six neurocognitive measures, suggesting a positive correlation between decreased blood perfusion and neurocognitive function impairment in patients with MTBI such as processing and response speed, memory, attention, word fluency (FAS), and executive functioning (Stroop) as shown in Figure 3. We did not find statistical significant correlations of neurocognitive function tests and averaged CBF in other brain regions except putamen, in which CBF correlates with executive functioning measured with Stroop test ($R^2 = 0.18$, P = 0.04).

DISCUSSION

MTBI represents one of our most important public health issues, with an incidence rate of well over a million people per year and various PCS associated symptoms following injury that are poorly understood. In this study we have focused on the thalamic injury in MTBI using high resolution True FISP ASL perfusion imaging. Our study provides evidence of hemodyanmic impairment in thalamic regions and these abnormalities in blood flow correlate with several neuropsychological measures, suggesting a cause for the persistent PCS in patients with extended period of MTBI.

The technique of ASL has been widely used for quantitative measurements of CBF as well as for detecting changes in blood flow associated with functional activation in the brain [27–30]. Compared to other modalities of investigating perfusion such as nuclear medicine techniques (PET, SPECT, Xe-CT) or DCE MRI, ASL offers advantages in that it is not limited by low spatial resolution and the use of exogenous endovascular contrast agents. However, most current methods of ASL are based on EPI, which introduces distortion artifacts and dephasing caused by local magnetic field inhomogeneity [37]. This is especially the case at higher fields, such that EPI at the basal ganglia level can be particularly challenging due to an increased iron component. Therefore, in this study we have used True FISP ASL [25], a non-EPI based method of ASL preparation which is a particularly attractive method of measuring local tissue perfusion in cerebral deep gray matter with high spatial resolution and without the distortion artifacts commonly associated with EPI based techniques [26].

We have focused on the thalamus in MTBI in this study because, as the centrally located relay station for information throughout the brain, it participates in communication among sensory, motor, and associative brain regions [6–9, 38]. Any small amount of damage may become amplified as it converges on this structure, influencing communication and synchronization among different areas. A number of histopathological studies have documented evidence of thalamic injury in TBI, including neuronal loss [39]. Natale et al. [40] demonstrated, in an experimental mouse model, that cortical damage could result in delayed remote thalamic neuron apoptosis using stereological techniques. However, the vast

majority of the cases cited above involve moderately and severely injured patients. Some of the authors contend that the thalamic injury is secondary while others believe it is primary; however none of these reports focus on MTBI or PCS.

Since viable brain tissue is highly dependent on its oxygen supply under normal and many pathologic circumstances [41], there is a general interest in studying the role of localized disturbances in CBF following TBI. Our study has demonstrated significantly lower CBF in both sides of thalamic regions in patients with MTBI as compared with normal controls, indicating a diffuse change of hemodynamic impairment in thalamus due to the injury. These results are in agreement with the hypothesis that functional blood flow abnormalities after brain injury are thought to contribute to posttraumatic neurocognitive and psychological sequelae [42]. There is also accumulating evidence indicating that regional ischemia plays a secondary role in patients with brain trauma [14, 43]. However, these perfusion abnormalities in the thalamic region have been poorly investigated in previous studies. We have also found significantly lower perfusion ($P = 0.03$) in patients in the right side of head of caudate nuclei and near significance ($P = 0.06$) in the left side of head of caudate nuclei. This may suggest the deep gray matter nuclei near the midline during the mild closed head injury are more vulnerable to damage during sudden acceleration or deceleration of the brain.

The median time since onset of brain injury in our patient group was 28.5 months, indicating that hemodynamic impairment can occur and persist in the extended phase of longstanding MTBI. Most of the human and animal studies conducted to date have acquired data during the initial 12 hours following injury, during which time it has been shown that ischemia occurs in 30% of the population [15–18]. However, our results are supported by experiments which have reported that reductions in CBF were observed in regions remotely distant from the impact site and can be present in a later phase after injury associated with delayed cognitive deficits [17, 19–21, 23]. For example, Kochanek et al. [24] reported blood perfusion impairment with delayed cognitive deficits at one year, suggesting a long-term effect of CBF on TBI. The perfusion changes in MTBI may be the result of a different set of mechanisms in the acute phase as compared to the subacute and chronic phase. Whereas hemodynamic abnormalities associated with the acute phase may be primary to the injury, arising, for example, from vasospasm and/or direct vascular injury, those decreases in perfusion associated with the extended phase may be secondary to the tissue injury, arising, for example, from a failure in cerebral autoregulation or a decrease of demand of blood supply. The decreased perfusion developed in the later phase of mild injury may be more responsible for the subsequent development of later symptoms associated with PCS. Therefore, in addition to the symptoms in the acute phase, these secondary symptoms due to late phase blood perfusion changes need to be addressed independently in order to prevent the additional late onset injury.

We also find significant correlations between the decrease of CBF in thalamic regions and neuropsychological dysfunction which involves multiple functional thalamic pathways that include processing speed, response speed, memory and learning, attention, verbal fluency and executive functioning deficits as shown in Table 3. These findings are consistent with the results of previous investigations that examined SPECT brain perfusion abnormalities associated with the most common clinical complaints and identified a greater number of focal areas exhibiting hypoperfusion in the basal ganglia and the thalamus [42, 44, 45]. We observed that our patient population differed significantly from normal controls in domains that included memory, executive functioning, and attention. A similar relationship between the thalamus and cognition has been described in several neurological diseases involving thalamic injury. For example, in a study of 22 patients with thalamic infarction, van der Werf et al. used experimental and established neuropsychological tests to demonstrate that

the thalamus plays a crucial role in memory, executive functioning, mental flexibility and attention [46]. In another example where the cholinergic system and cognitive sequelae in a group of moderate-severe head injury survivors were investigated in a recent study, the patients showed deficits in sustained attention and impaired associate learning and reaction time compared with a group of controls, and these cognitive skills were shown to depend on the integrity of the cholinergic system found in the bilateral hippocampal formation and the thalamus. Interestingly, this study using voxel-based morphometry also revealed reduced gray matter density in the thalamus [47]. Another recent SPECT study examining the neuropsychological performance of CBF deficits in patients with left anterior thalamic infarction by Shim et al. [48], found similar deficits in memory, word fluency, and executive functioning (Stroop). These three examples from the literature together with the findings of our study suggest that thalamic injury does occur in MTBI and that damage to the thalamus leads to neurocognitive functional deficits. An understanding of the significance of thalamic injury and how it relates to the symptoms of MTBI promises to fill an important void in our knowledge of this disorder.

There are several limitations in the current study. Although true FISP ASL provides high resolution perfusion imaging, the current setting only allows one single slice to measure CBF in the thalamus. It potentially provides more slices within a similar time frame at higher field MR due to the increased signal to noise. However, the focus of this study was to investigate the role of small localized disturbances in CBF in the basal ganglia regions that include both deep gray matter nuclei and white matter, where the standard representative regions of interest were selected and compared in both patients and controls. Another concern is that this study lacks acute phase data, however, a longitudinal study, which is currently planned, will warrant the complete data.

CONCLUSIONS

True FISP ASL indicates that a state of hypoperfusion may exist in the thalamus in chronic symptomatic patients following MTBI. Such hemodynamic impairment can occur and persist in patients with relatively longstanding MTBI and the extent is more severe in thalamus regions than white matter and other basal ganglia regions, which may help to better understand the complex persistent postconcussive syndrome in patients with MTBI.

Acknowledgments

References

1. Ryan LM, Warden DL. Post concussion syndrome. Int Rev Psychiatry. 2003; 15(4):310–6. [PubMed: 15276952]

2. Levin HS, Mendelsohn D, Lilly MA, et al. Magnetic resonance imaging in relation to functional outcome of pediatric closed head injury: a test of the Ommaya-Gennarelli model. Neurosurgery. 1997; 40(3):432–40. discussion 440–1. [PubMed: 9055281]

3. Lishman WA. Physiogenesis and psychogenesis in the 'post-concussional syndrome'. Br J Psychiatry. 1988; 153:460–9. [PubMed: 3074853]

4. Brown SJ, Fann JR, Grant I. Postconcussional disorder: time to acknowledge a common source of neurobehavioral morbidity. J Neuropsychiatry Clin Neurosci. 1994; 6(1):15–22. [PubMed: 8148632]

5. Jane JA, Steward O, Gennarelli T. Axonal degeneration induced by experimental noninvasive minor head injury. J Neurosurg. 1985; 62(1):96–100. [PubMed: 3964861]

6. Crosson B, Hughes CW. Role of the thalamus in language: is it related to schizophrenic thought disorder? Schizophr Bull. 1987; 13(4):605–21. [PubMed: 3326161]

7. Steriade, M.; Jones, EG.; McCormick, D. Thalamus. Amsterdam ; New York: Elsevier; 1997.

8. Guillery RW. Anatomical evidence concerning the role of the thalamus in corticocortical communication: a brief review. J Anat. 1995; 187 (Pt 3):583–92. [PubMed: 8586557]

9. O'Leary DD, Schlaggar BL, Tuttle R. Specification of neocortical areas and thalamocortical connections. Annu Rev Neurosci. 1994; 17:419–39. [PubMed: 8210182]

10. Coles JP. Regional ischemia after head injury. Curr Opin Crit Care. 2004; 10(2):120–5. [PubMed: 15075722]

11. Miller JD. Head injury and brain ischaemia--implications for therapy. Br J Anaesth. 1985; 57(1): 120–30. [PubMed: 3881110]

12. Graham DI, Adams JH. Ischaemic brain damage in fatal head injuries. Lancet. 1971; 1(7693):265–6. [PubMed: 4100017]

13. Schroder ML, Muizelaar JP, Bullock MR, Salvant JB, Povlishock JT. Focal ischemia due to traumatic contusions documented by stable xenon-CT and ultrastructural studies. J Neurosurg. 1995; 82(6):966–71. [PubMed: 7760199]

14. Bonne O, Gilboa A, Louzoun Y, et al. Cerebral blood flow in chronic symptomatic mild traumatic brain injury. Psychiatry Res. 2003; 124(3):141–52. [PubMed: 14623066]

15. Yamakami I, McIntosh TK. Effects of traumatic brain injury on regional cerebral blood flow in rats as measured with radiolabeled microspheres. J Cereb Blood Flow Metab. 1989; 9(1):117–24. [PubMed: 2910893]

16. Bryan RM Jr, Cherian L, Robertson C. Regional cerebral blood flow after controlled cortical impact injury in rats. Anesth Analg. 1995; 80(4):687–95. [PubMed: 7893019]

17. Kochanek PM, Marion DW, Zhang W, et al. Severe controlled cortical impact in rats: assessment of cerebral edema, blood flow, and contusion volume. J Neurotrauma. 1995; 12(6):1015–25. [PubMed: 8742130]

18. Biagas KV, Grundl PD, Kochanek PM, Schiding JK, Nemoto EM. Posttraumatic hyperemia in immature, mature, and aged rats: autoradiographic determination of cerebral blood flow. J Neurotrauma. 1996; 13(4):189–200. [PubMed: 8860199]

19. Hovda DA, Lee SM, Smith ML, et al. The neurochemical and metabolic cascade following brain injury: moving from animal models to man. J Neurotrauma. 1995; 12(5):903–6. [PubMed: 8594218]

20. Forbes ML, Hendrich KS, Kochanek PM, et al. Assessment of cerebral blood flow and CO_2 reactivity after controlled cortical impact by perfusion magnetic resonance imaging using arterial spin-labeling in rats [published erratum appears in J Cereb Blood Flow Metab 1997 Nov;17(11): 1263]. J Cereb Blood Flow Metab. 1997; 17(8):865–74. [PubMed: 9290584]

21. Bramlett HM, Dietrich WD, Green EJ. Secondary hypoxia following moderate fluid percussion brain injury in rats exacerbates sensorimotor and cognitive deficits. J Neurotrauma. 1999; 16(11): 1035–47. [PubMed: 10595820]

22. Dixon CE, Kochanek PM, Yan HQ, et al. One-year study of spatial memory performance, brain morphology, and cholinergic markers after moderate controlled cortical impact in rats. J Neurotrauma. 1999; 16(2):109–22. [PubMed: 10098956]

23. Dietrich WD, Alonso O, Busto R, et al. Widespread hemodynamic depression and focal platelet accumulation after fluid percussion brain injury: a double-label autoradiographic study in rats. J Cereb Blood Flow Metab. 1996; 16(3):481–9. [PubMed: 8621753]

24. Kochanek PM, Hendrich KS, Dixon CE, Schiding JK, Williams DS, Ho C. Cerebral blood flow at one year after controlled cortical impact in rats: assessment by magnetic resonance imaging. J Neurotrauma. 2002; 19(9):1029–37. [PubMed: 12482116]

25. Martirosian P, Klose U, Mader I, Schick F. FAIR true-FISP perfusion imaging of the kidneys. Magn Reson Med. 2004; 51(2):353–61. [PubMed: 14755661]

26. Grossman, E.; Chen, Q.; An, J., et al. Measurement of Deep Gray Matter Perfusion Using a Segmented True FISP ASL Method at 3T. ISMRM; Berlin: 2007.

27. Detre JA, Leigh JS, Williams DS, Koretsky AP. Perfusion imaging. Magn Reson Med. 1992; 23(1):37–45. [PubMed: 1734182]

28. Edelman RR, Siewert B, Darby DG, et al. Qualitative mapping of cerebral blood flow and functional localization with echo-planar MR imaging and signal targeting with alternating radio frequency. Radiology. 1994; 192(2):513–20. [PubMed: 8029425]

29. Kim SG. Quantification of relative cerebral blood flow change by flow-sensitive alternating inversion recovery (FAIR) technique: application to functional mapping. Magn Reson Med. 1995; 34(3):293–301. [PubMed: 7500865]

30. Kwong KK, Chesler DA, Weisskoff RM, et al. MR perfusion studies with T1-weighted echo planar imaging. Magn Reson Med. 1995; 34(6):878–87. [PubMed: 8598815]

31. Yang Y, Frank JA, Hou L, Ye FQ, McLaughlin AC, Duyn JH. Multislice imaging of quantitative cerebral perfusion with pulsed arterial spin labeling. Magn Reson Med. 1998; 39(5):825–32. [PubMed: 9581614]

32. Clare S, Jezzard P. Rapid T(1) mapping using multislice echo planar imaging. Magn Reson Med. 2001; 45(4):630–4. [PubMed: 11283991]

33. Lu H, Nagae-Poetscher LM, Golay X, Lin D, Pomper M, van Zijl PC. Routine clinical brain MRI sequences for use at 3. 0 Tesla. J Magn Reson Imaging. 2005; 22(1):13–22. [PubMed: 15971174]

34. Figueiredo PM, Clare S, Jezzard P. Quantitative perfusion measurements using pulsed arterial spin labeling: effects of large region-of-interest analysis. J Magn Reson Imaging. 2005; 21(6):676–82. [PubMed: 15906323]

35. Buxton RB, Frank LR, Wong EC, Siewert B, Warach S, Edelman RR. A general kinetic model for quantitative perfusion imaging with arterial spin labeling. Magn Reson Med. 1998; 40(3):383–96. [PubMed: 9727941]

36. Lu H, Clingman C, Golay X, van Zijl PC. Determining the longitudinal relaxation time (T1) of blood at 3. 0 Tesla. Magn Reson Med. 2004; 52(3):679–82. [PubMed: 15334591]

37. Weiskoff, R.; Cohen, M. Echo planar imaging: technology and techniques. In: Bradley, WJ.; Chen, D.; Atkinson, D., et al., editors. Magnetic Resonance Imaging. 3. St Louis: Mosby-Year Book; 1997. p. 125-157.

38. Sherman SM, Guillery RW. Functional organization of thalamocortical relays. J Neurophysiol. 1996; 76(3):1367–95. [PubMed: 8890259]

39. Ross DT, Graham DI, Adams JH. Selective loss of neurons from the thalamic reticular nucleus following severe human head injury. J Neurotrauma. 1993; 10(2):151–65. [PubMed: 8411218]

40. Natale JE, Cheng Y, Martin LJ. Thalamic neuron apoptosis emerges rapidly after cortical damage in immature mice. Neuroscience. 2002; 112(3):665–76. [PubMed: 12074908]

41. Ichimi K, Kuchiwaki H, Inao S, Shibayama M, Yoshida J. Cerebral blood flow regulation under activation of the primary somatosensory cortex during electrical stimulation of the forearm. Neurol Res. 1999; 21(6):579–84. [PubMed: 10491820]

42. Abu-Judeh HH, Singh M, Masdeu JC, Abdel-Dayem HM. Discordance between FDG uptake and technetium-99m-HMPAO brain perfusion in acute traumatic brain injury. J Nucl Med. 1998; 39(8):1357–9. [PubMed: 9708506]

43. Bouma GJ, Muizelaar JP, Stringer WA, Choi SC, Fatouros P, Young HF. Ultra-early evaluation of regional cerebral blood flow in severely head-injured patients using xenon-enhanced computerized tomography. J Neurosurg. 1992; 77(3):360–8. [PubMed: 1506882]

44. Abdel-Dayem HM, Abu-Judeh H, Kumar M, et al. SPECT brain perfusion abnormalities in mild or moderate traumatic brain injury. Clin Nucl Med. 1998; 23(5):309–17. [PubMed: 9596157]

45. Nakamizo A, Inamura T, Amano T, et al. Decreased thalamic metabolism without thalamic magnetic resonance imaging abnormalities following shearing injury to the substantia nigra. J Clin Neurosci. 2002; 9(6):685–8. [PubMed: 12604285]

46. Van der Werf YD, Witter MP, Uylings HB, Jolles J. Neuropsychology of infarctions in the thalamus: a review. Neuropsychologia. 2000; 38(5):613–27. [PubMed: 10689038]

47. Salmond CH, Chatfield DA, Menon DK, Pickard JD, Sahakian BJ. Cognitive sequelae of head injury: involvement of basal forebrain and associated structures. Brain. 2005; 128(Pt 1):189–200. [PubMed: 15548553]

48. Shim YS, Kim JS, Shon YM, Chung YA, Ahn KJ, Yang DW. A serial study of regional cerebral blood flow deficits in patients with left anterior thalamic infarction: Anatomical and neuropsychological correlates. J Neurol Sci. 2008; 266(1–2):84–91. [PubMed: 18031760]
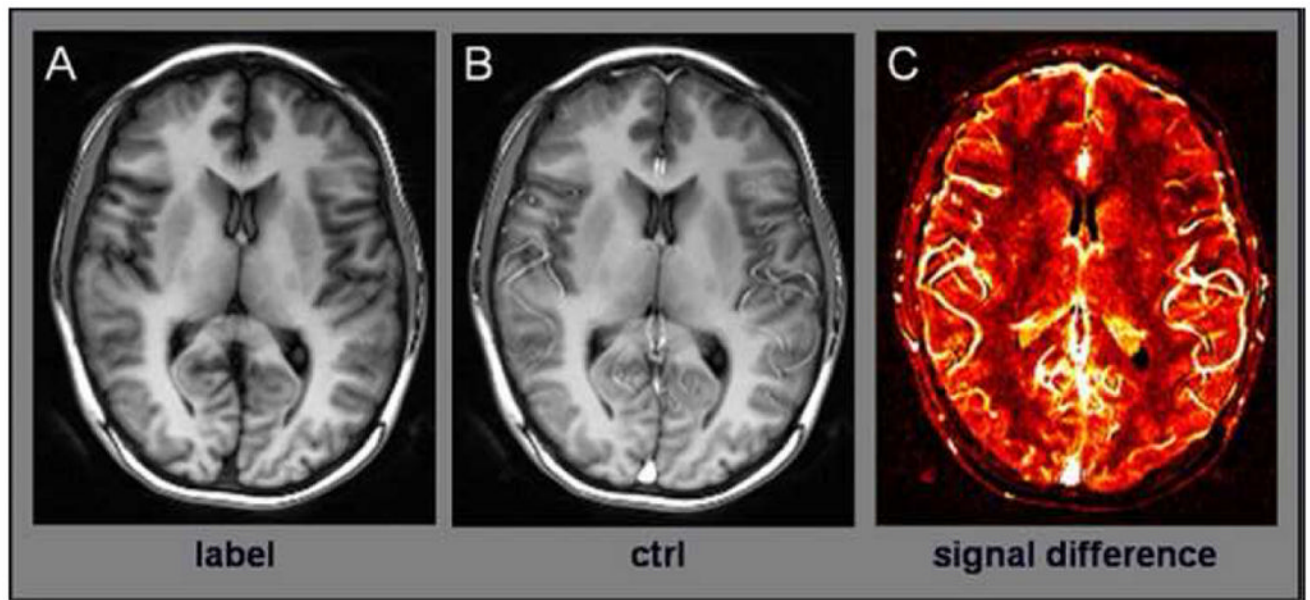
Figure 1.
An example of True FISP ASL images showing labeled and control images (A and B) obtained using the current technique. The control image has high signal intensity due un-inverted blood flow entering tissue space. The difference of the two images (C) is a relative map of cerebral blood flow. Note that signal difference is higher in the gray matter than in the white matter. Measurements of regional CBF are made in frontal white matter and deep gray matter regions including thalamus, putamen, and caudate nuclei.
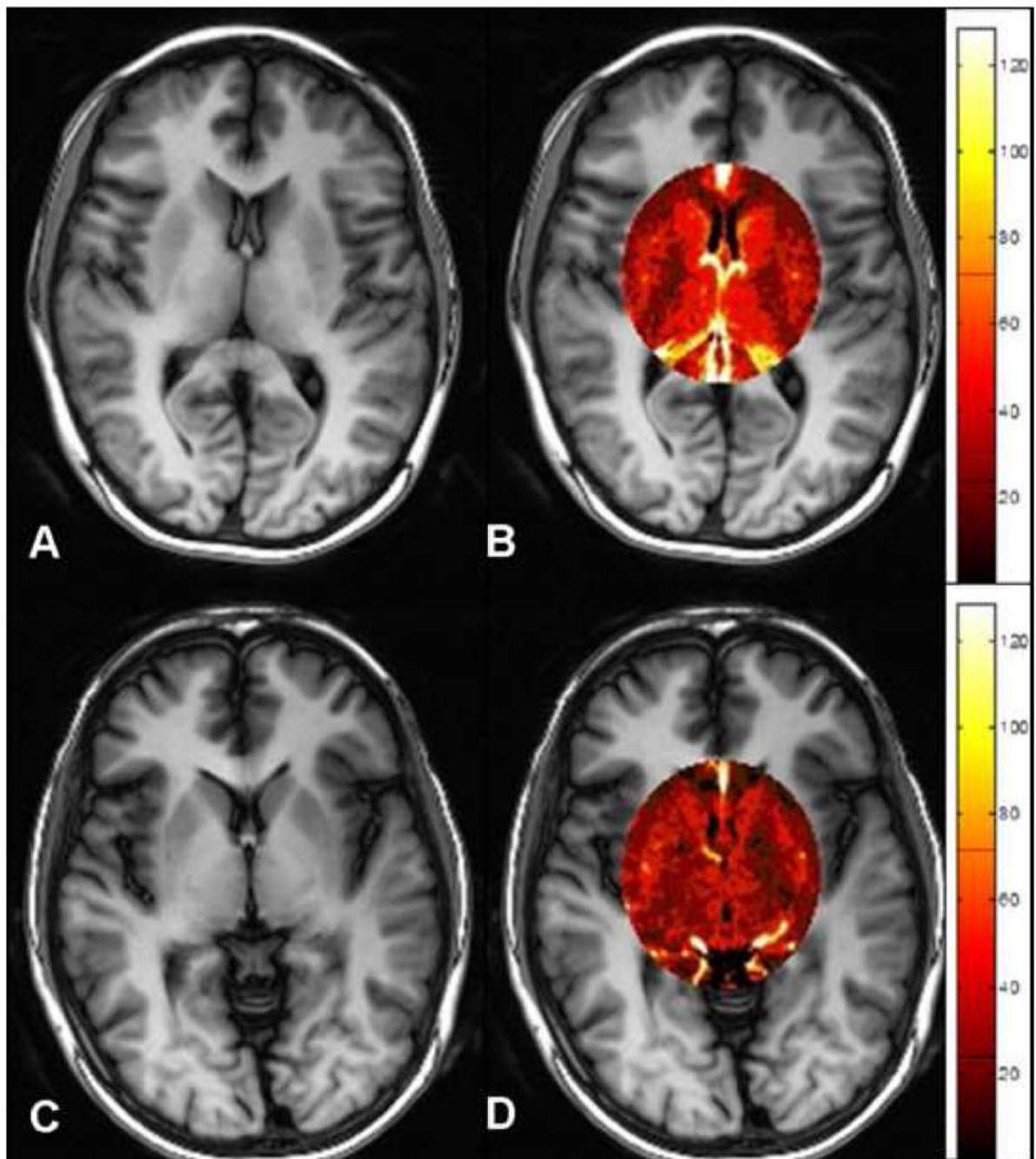
Figure 2.
True FISP ASL perfusion images and regional maps in an age-matched normal control (A, B) and in a patient (C, D). Note the decreased level of CBF within the selected region in the patient (D) as compared to the normal control (B).
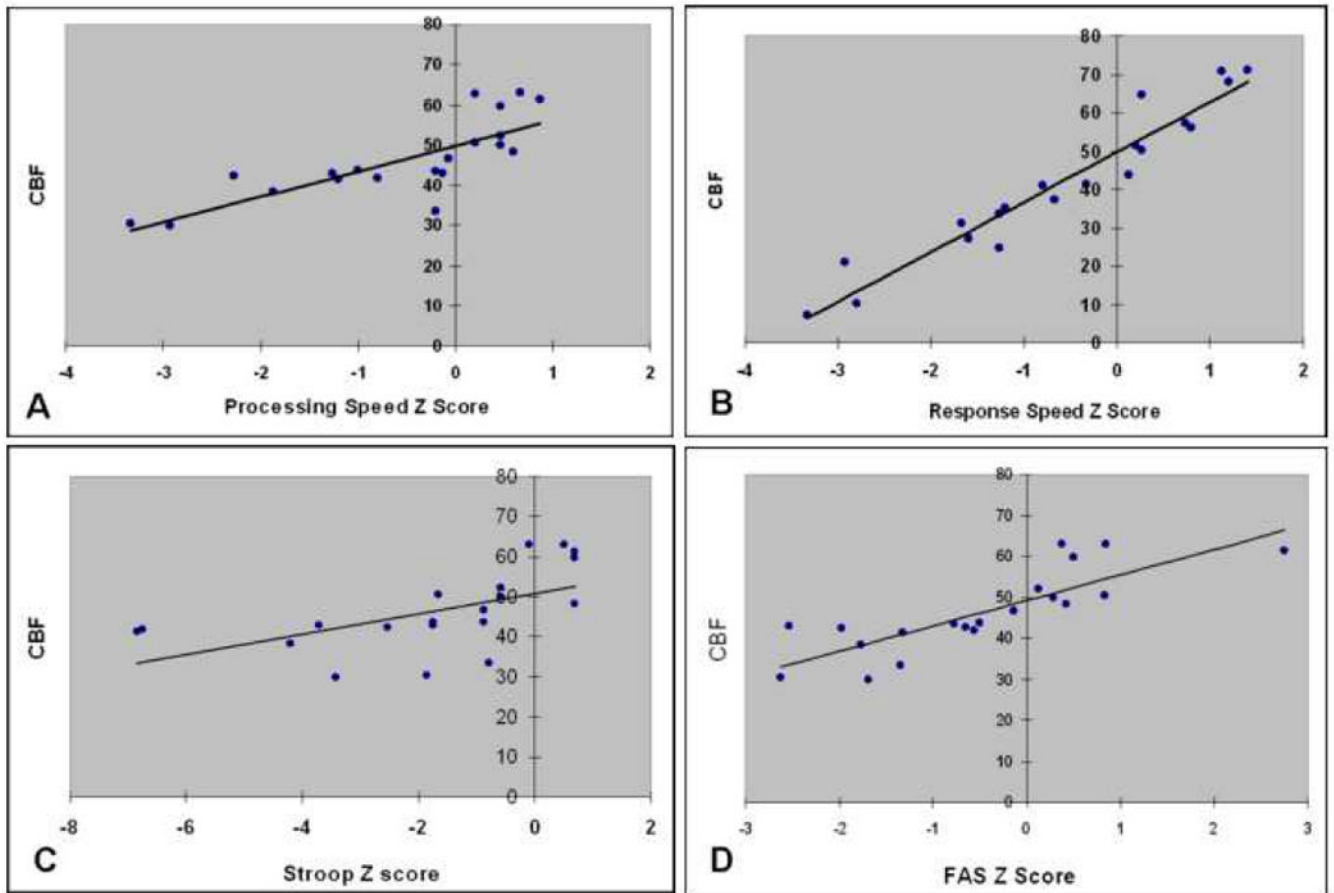
Figure 3.
Regression analyses have shown a positive correlation between averaged CBF from both sides in thalamic regions and several neuropsychological functions computed as standardized z score such as processing ($R^2 = 0.59$, $p < 0.0001$) and response speed ($R^2 = 0.72$, $P < 0.0001$), Stroop ($R^2 = 0.26$, $P = 0.01$) and verbal fluency (FAS) tests ($R^2 = 0.66$, $P < 0.0001$).

Table 1

The mean and standard deviation (SD) of CBF (ml/100g tissue/min) measure in different brain regions among patients and controls assessed with an unequal variance t test (T).

Regions	Side	Controls	MTBI	P-value
Thalamus	Right	59.7 ± 13.3	46.9 ± 10.4	**0.002**
	Left	55.2 ± 9.7	45.0 ± 9.7	**0.002**
	Both	57.4 ± 10.3	45.9 ± 9.8	**0.001**
Putamen	Right	51.2 ± 14.7	50.5 ± 8.3	0.84
	Left	47.1 ± 11.5	45.4 ± 7.8	0.61
	Both	48.0 ± 11.9	49.5 ± 8.1	0.67
Caudate	Right	63.5 ± 13.6	53.7 ± 12.8	**0.03**
	Left	55.8 ± 14.8	50.1 ± 14.7	0.06
	Both	58.1 ± 15.3	51.9 ± 12.4	**0.02**
Frontal WM	Right	24.3 ± 7.4	23.0 ± 7.4	0.59
	Left	25.1 ± 7.8	22.5 ± 6.0	0.26
	Both	24.3 ± 7.2	23.2 ± 6.7	0.65

Table 2

The mean and standard deviation (SD) of neurocognitive tests (z score) in patients and controls assessed with an unequal variance t test (T).

Neuropsych Tests	Control		MTBI		P-value
	Mean	SD	Mean	SD	
Processing Speed	0.29	0.48	−0.56	1.20	**0.004**
Response Speed	0.58	0.81	−0.64	1.40	**0.002**
Memory/Learning	0.39	1.09	−0.35	1.64	0.11
Attention	0.28	0.85	−0.30	1.28	0.11
Similarities Category	0.19	0.85	−0.29	1.28	0.17
Similarities Shift	−0.50	1.00	−0.58	1.68	0.86
Cancellation Error	0.10	0.79	−0.64	1.10	**0.021**
Cancellation Time	0.14	0.82	−0.10	1.23	0.46
Verbal Fluence (FAS)	0.49	0.87	−0.57	1.29	**0.003**
Stroop	0.26	0.55	−1.73	2.19	**0.0006**

Table 3

Significant correlations (adjusted R^2, P 0.01) between CBF measured in thalamic regions (right, left and both sides) and neurocognitve tests in patients with MTBI.

Neuropsych Tests	CBF Measurement		
	Right Side	Left Side	Average
Processing Speed	0.60	0.51	0.59
Response Speed	0.72	0.64	0.72
Memory	0.47	0.37	0.44
Cancellation Error	0.46	0.55	0.54
Verbal Fluency (FAS)	0.67	0.58	0.66
Stroop	0.32	0.18	0.26